

THE EARLY JURASSIC OIL SHALES IN THE QIANGTANG BASIN, NORTHERN TIBET: BIOMARKERS AND TOARCIC OCEANIC ANOXIC EVENTS

HAISHENG YI^(a,b), LAN CHEN^{(c,d)*}, HUGH C. JENKYN^(d),
XUEJUAN DA^(c), MINQUAN XIA^(c), GUIWEN XU^(c),
CHANGJUN JI^(b)

- (a) State Key Laboratory of Oil/Gas Reservoir Geology and Exploitation, Chengdu University of Technology, Chengdu 610059, China
(b) Institute of Sedimentary Geology, Chengdu University of Technology, Chengdu 610059, China
(c) College of Petroleum Engineering, Chongqing University of Science and Technology, Chongqing 401331, China
(d) Department of Earth Sciences, University of Oxford, South Parks Road, Oxford OX1 3AN, United Kingdom

Abstract. In the Qiangtang Basin, northern Tibet, the most complete and extensive marine sedimentary strata outcropped in the Shuanghu-Sewa-Amdo area during the Jurassic, especially the Early Jurassic. The organic-rich marine sediments – commonly referred to as black shales – were deposited in the Early Jurassic, therefore, many petroleum geologists have been focusing on them for many years. Although achievements in geological investigations and petroleum resource assessments during recent years have been remarkable, the environmental conditions, mechanics, and process that resulted in the deposition of high-organic sediments during the Early Toarcian (183–176.5 Ma, Early Jurassic) Oceanic Anoxic Event are still a matter of discussions. In this paper, we deal with the biomarker distributions of Lower Jurassic oil shales in the Biluo Co section, Shuanghu area of northern Tibet. The oil shales are characterized by a marked predominance of short chain n-alkanes with a maximum at C₁₆ or C₁₇, nC₁₇/nC₃₁ ratio values between 9.4 and 17.8, and low Pr/Ph ratios. Furthermore, a series of C₂₇ and C₂₉–C₃₅ hopanes with minor amounts of gammacerane are present in all samples, as indicated by gammacerane/C₃₀-17 α -hopane values from 0.06 to 0.12 and the steranes C₂₇/C₂₉ ratios higher than 1 in the three samples. The above-mentioned parameters indicate that the organic matter source is attributed to an algal/bacterial contribution. According to maturity parameters, all the homohopane 22S/(22S+22R) values in this study are > 0.58 and the sterane 20S/(20S+20R) values are all between 0.48 and 0.59, which is consistent

* Corresponding author: e-mail cllc-10@163.com

with a higher level of thermal maturity. Widespread anoxia led to the deposition of organic-rich sediments that removed isotopically light carbon from the oceans and drove carbon-isotope ratios to higher values with a positive excursion close to 2.17‰. From biomarker distributions, the differences in $\delta^{13}\text{C}_{\text{kerogen}}$ are related to the difference in $\delta^{13}\text{C}$ of CO_2 in the photic zone rather than the organic matter compositions.

Keywords: Early Jurassic oil shales, biomarkers, Toarcian Oceanic Anoxic Event, northern Tibet.

1. Introduction

The Early Toarcian Oceanic Anoxic Event (OAE), as defined by both relatively high total organic carbon (TOC) values and ammonite and nannofossil biostratigraphy, is clearly synchronous across Europe and will undoubtedly prove to be so in global context [1]. Generally speaking, the most organic carbon-rich Toarcian shales have a good to excellent oil-generation potential [2]. Therefore, petroleum geologists have been focusing on these shales in the Tethyan sea as important petroleum source rocks [3]. Organic-rich shales certainly appear from literature sources to be common in the Toarcian, but it is not clear whether this is because they have been reported on assiduously because of their intrinsic interest, or because they really do represent a high proportion of all Toarcian strata, or because the definition of black shale is stretch beyond breaking point [4–5]. Nevertheless, a negative carbon-isotope excursion between -5‰ and -7‰ (PDB) has been reported from the Boreal (NW European) *falciferum* Zone [6–9]. This carbon-isotope excursion has been ascribed to the release, in discrete stepwise pulses, of isotopically light carbon into the ocean-atmosphere system [9]. In contrast, the positive carbon-isotope excursion associated with the Early Toarcian OAE has been attributed to an increased sequestration of isotopically light marine organic matter in ocean sediments under oxygen-depleted conditions, leading to the corresponding ‘heavy’ signal preserved in bulk rock, belemnite calcite, marine organic matter, and wood [6–7, 10–14]. This interpretation is supported by the widespread occurrence of organic-rich black shales, and from biomarker evidence for photic-zone sulphate reduction in horizons that show this organic enrichment [2, 15–16]. However, what is still poorly known about this event is its manifestation in non-marine and marginal marine environments.

As mentioned above, several studies focusing on the carbon-isotope excursions and possible causative mechanisms have been undertaken in NW Europe and western Tethyan areas. However, a detailed research is not available for the Toarcian black shales of the eastern Tethyan area in the literature, especially the Qiangtang Basin, northern Tibet (China). The Biluo Co section in the Qiangtang Basin was characterized by grey to dark-colored alternating oil shales, marls and mudstones with a positive excursion close to

2.17‰ [17], which have been associated with other Early Toarcian Oceanic Anoxic Events (OAEs) in Europe. Therefore, the objective of this study was to test if the positive carbon isotope excursion of the organic carbon of the Biluo Co shales can be attributed to heavy CO₂ recycled into the marine organic matter from stagnate waters. To test this explanation, this paper chooses biomarker evidence that shows this organic enrichment and an effect on Toarcian OAE.

2. Geological background

The Qiangtang Basin lies in between the Jinshajiang suture zone (JSS) and the Banggong-Nujiang suture zone (BNS), in the central Qinghai-Tibet Plateau (Fig. 1a). Structurally, the basin is characterized by one uplift and two depressions. From north to south, they are the northern Qiangtang depression, central uplift and southern Qiangtang depression, respectively [18–19] (Fig. 1b). Jurassic strata are the most complete and extensive marine deposits in the basin. We carried out detailed field investigations of the Shuanghu oil shales section in the southeastern Biluo Co area, which is about 45 km away from the Shuanghu special district (Fig. 1b). The Biluo Co section crops out on the margin of the central uplift. The whole succession has been described in detail previously by Chen et al. (2005, 2012) [17, 20] with oil shales, shales, marls, and mudstones (Fig. 1c). In 1994, 2003 and 2011, our research teams surveyed this section again and again, and found abundant Jurassic bivalves and ammonites as well as basalts in the lower parts. Abundant ammonites at the top of the section include a specimen identified as an Early Toarcian *Harpoceras* sp., which is related to the global oceanic anoxic event during the peak of transgression in the Early Jurassic [17].

3. Samples and methods

All 4 samples are oil shales which were collected from the Biluo Co section and used for biomarkers. From lower to upper, the samples are marked as BL-1, BL-2, BL-3 and BL-4 (Fig. 1c). Bulk parameters determined at regular intervals over the section reveal that TOC contents in the black shales are generally high, between 1.86% and 26.1% [17]. The samples were first washed thoroughly with dichloromethane (DCM) to remove possible contamination from the surface and ground to < 200 mesh. All experiments were carried out in Yangtze University, China.

Each sample was reacted with DCM for 72 h in a Soxhlet apparatus. The solvent was removed by rotary evaporation and the residue dissolved in cyclohexane. Asphaltenes were removed by centrifugal precipitation with chilled *n*-heptane (at least 40 x v/v). Aliquots of maltenes were separated by

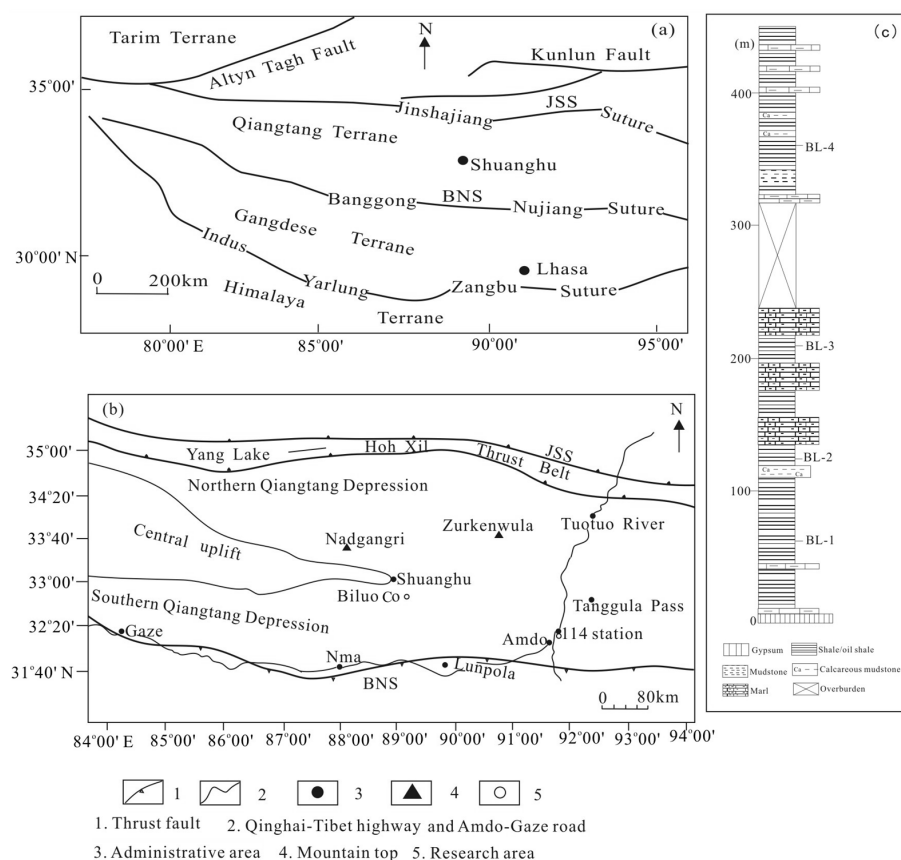


Fig. 1. Tectonic sketch map of the Qinghai-Tibet plateau (a) showing the tectonic units of Qiangtang Basin and location of Biluo Co area (b); (c) is the lithological column with sampling locations.

silica gel chromatography using hexane to elute the saturated hydrocarbons, 4:1 hexane:DCM for the aromatic hydrocarbons and 1:2 DCM:MeOH for the polar fraction. Activated Cu was added to the saturate fraction to remove elemental sulfur and the fraction was further separated into straight chain and branched/cyclic hydrocarbons using the 5Å molecular sieve (Merck, Germany).

Gas chromatography-mass spectrometry (GC-MS) was performed using a Micromass Platform LC mass spectrometer equipped with an HP 6890 gas chromatograph. For the saturated hydrocarbons, a 30 m HP-5 fused silica column (0.25 mm i.d., 0.25 µm film thickness) was used with He as the carrier gas. The oven temperature programme was: 65 °C (1 min) to 290 °C (held 30 min) at 3 °C/min. The transfer line temperature was 250 °C and the ion source temperature 200 °C. The ion source was operated in the electron impact mode at 70 eV.

4. Results

Several biomarkers, including *n*-alkanes, acyclic isoprenoids, terpenoids and steroids, were detected in all samples (Figs. 2, 3, 4 and Table).

4.1. *n*-alkanes and acyclic isoprenoids

The samples are generally dominated by C₁₂ to C₃₅ *n*-alkanes maximizing at C₁₆ or C₁₇ (Fig. 2). There is a marked presence of short chain *n*-alkanes with essentially no odd/even predominance (OEP; 0.91 to 1.06) and a carbon preference index (CPI) of 1.05 (Table 1). In addition, the stratigraphic variation in nC₁₇/nC₃₁, nC₂₁⁻/nC₂₂⁺ and nC₂₁+nC₂₀/nC₂₈+nC₂₉ alkanes is shown in Table 1, indicating the predominance of light hydrocarbons.

The acyclic isoprenoids dominated by pristane (Pr) and phytane (Ph) were detected in all samples (Fig. 2). Pr/Ph values range from 0.67 to 1.31, Pr/nC₁₇ from 0.3 to 0.53, and Ph/nC₁₈ from 0.32 to 0.56 (Table).

4.2. Terpenoids

The *m/z* 191 chromatograms are shown in Figure 3. The most abundant hopanes were C₂₉ and C₃₀ through the whole strata, but C₂₇ hopanes (Ts, 18 α -22,29,30-trinorneohopane and Tm, 17 α -22,29,30-trinorhopane) were subordinate. C₃₁ to C₃₅ homohopanes were also detected, although in low abundance. Gammacerane occurred in lower abundance, and oleanane and lupane were detected in none of the samples. In contrast, tricyclic terpanes were represented by a series from C₁₉–C₃₀, and only C₂₄ was present in tetracyclic terpanes. No methyl hopanoids, which originate from cyanobacteria, were detected in *m/z* 205 chromatograms, although shales from offshore West Africa (upper two panels), and Green River (U.S.A), and Serpiano (Switzerland) shales show the 2 α - and 3 β -methylhopanes derived [22–24] from distinct bacterial sources: cyanobacteria (2-methyl) and methanotrophic bacteria (3-methyl). The 25-norhopanoids, however, occurred in *m/z* 177 mass chromatograms. Without exception, some classic 25-norhopanes were recognized, such as 17 α ,21 β -25,30-dinorhopane, 17 β ,21 α -25,30-dinormoretane, 17 α , 21 β -25-norhopane, and 17 β , 21 α -25-normoretane. Blanc and Connan [25] considered the 25-norhopanes as a palaeobiodegradation indicator in oil apparently non-biodegraded oil. Furthermore, 25-norhopanes appear to be diagnostic of specific environmental conditions (marine and lacustrine source rocks, dysoxic and not highly hypersaline).

4.3. Steroids

Besides the regular steranes (C₂₇–C₂₉) and diasteranes (C₂₇–C₂₉), a series of 4-methyl steranes (C₂₈–C₃₀) and abundant pregnanes (C₂₁–C₂₂) were detected in the *m/z* 217 chromatograms (Fig. 4). Furthermore, the regular steranes show a V-type distribution with variable values from 0.92 to 1.33 for the $\Sigma C_{27}/\Sigma C_{29}$ ratio, and 0.53 to 0.60 for the $\Sigma C_{28}/\Sigma C_{29}$ ratio through the section.

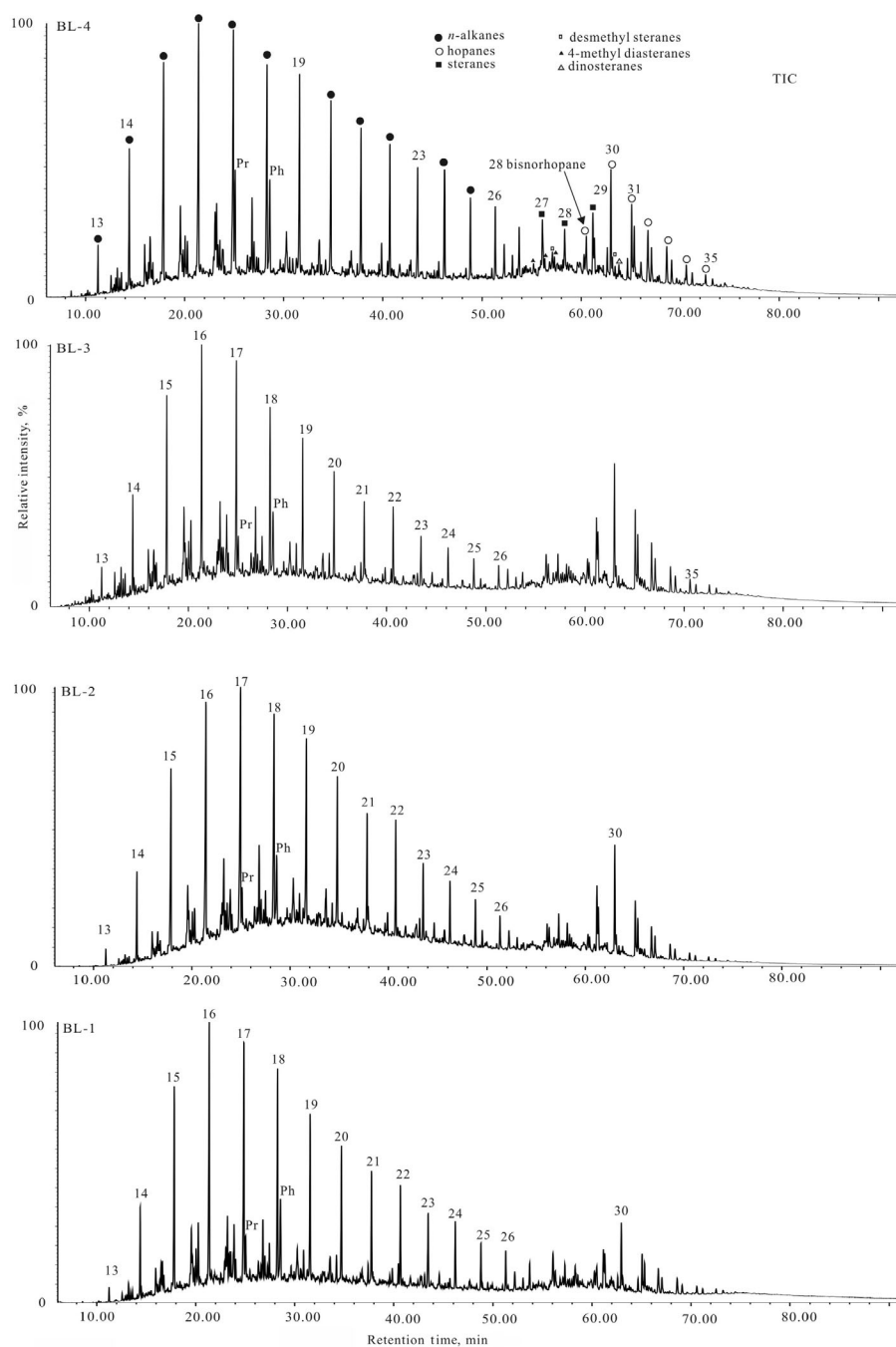


Fig. 2. Total ion chromatograms (TIC) showing the relative abundance of *n*-alkanes, regular isoprenoids, hopanes and steranes of the black shales from the studied section. Numbers above the symbols denote carbon number.

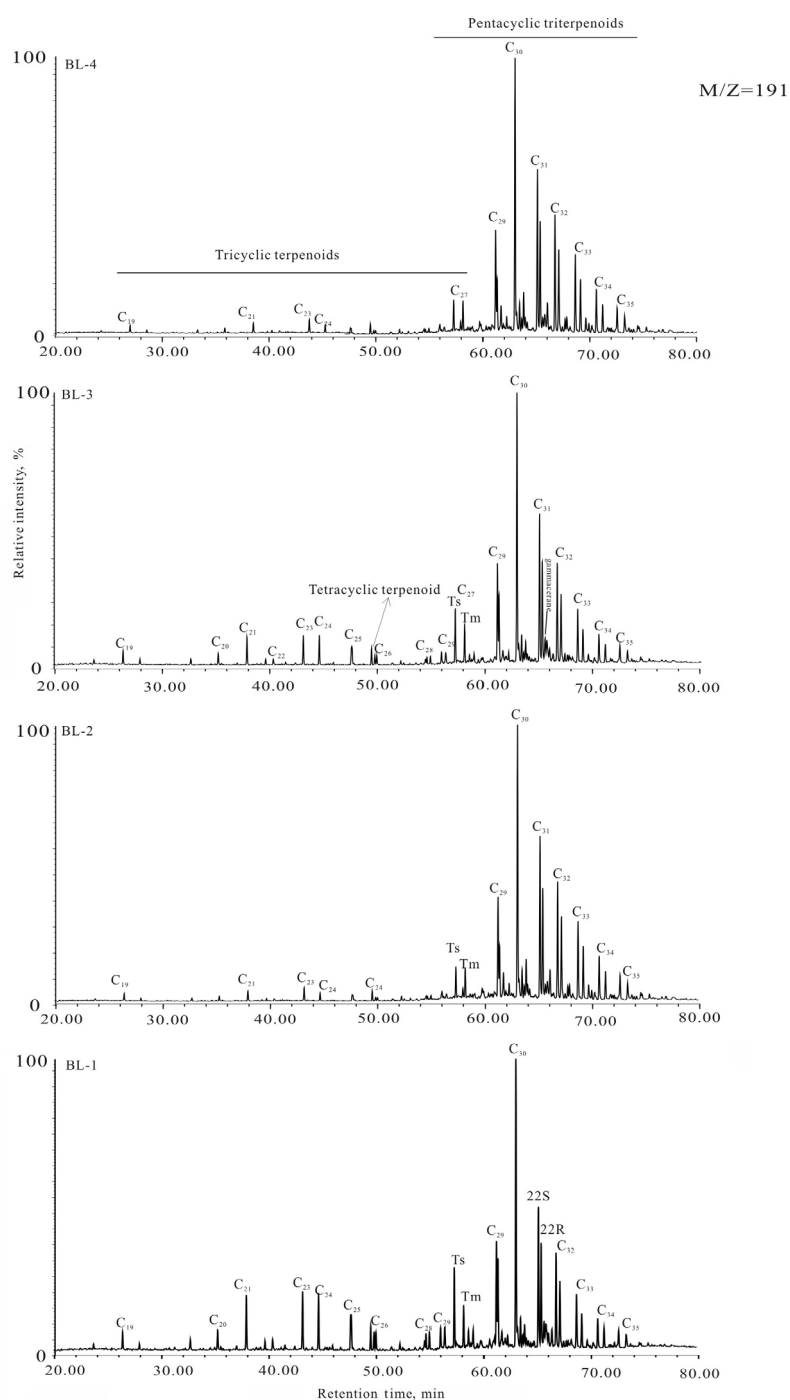


Fig. 3. The m/z 191 chromatograms showing the relative abundance of terpenoids in the representative samples. Ts, 18 α (H)-22,29,30-trisnorneohopane; Tm, 17 α (H)-22,29,30-trisnorneohopane. The 22S and 22R epimers are shown for C₃₁-homohopanes.

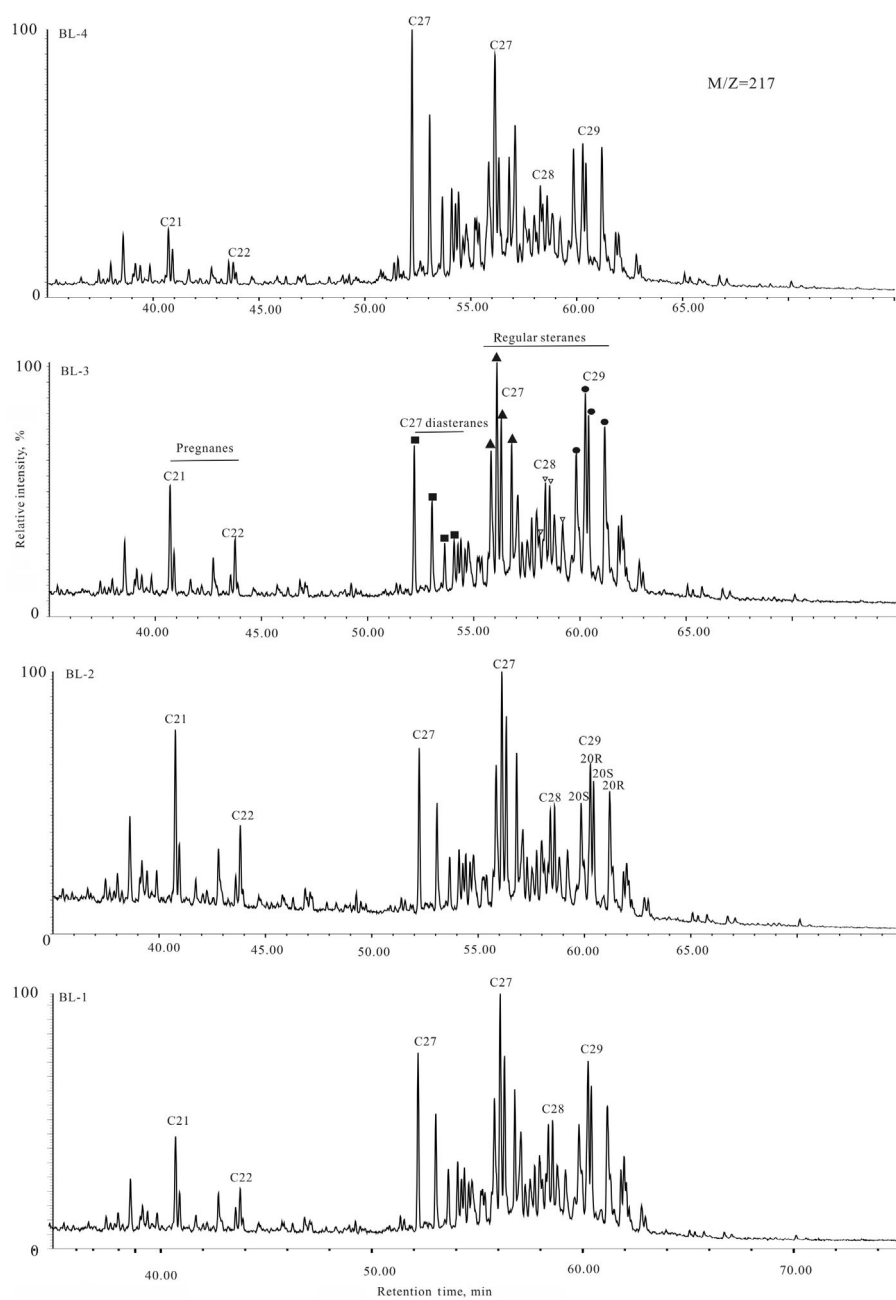


Fig. 4. The m/z 217 chromatograms showing the relative abundance of steriods in the representative samples. The 20S and 20R epimers are shown for C₂₉ regular steranes.

Table. Biomarker parameters based on *n*-alkanes, acyclic isoprenoids, terpenoids and steroids of oil shales from Biluo Co section, Shuanghu area of northern Tibet

Sample	<i>n</i> -alkanes					Isoprenoids			Steranes				Hopanes		
	Main peak	OEP ^a	CPI ^b	nC ₁₇ /nC ₃₁	nC ₂₁ */nC ₂₂ +	Pr/Ph	Pr/nC ₁₇	Ph/nC ₁₈	Pregnane/C ₂₉ -20R	Dia- Σ C ₂₇ /Reg- Σ C ₂₇	Reg- Σ C ₂₇ / Σ C ₂₉	C ₂₉ $\alpha\alpha\alpha$ 20S/(20S+20R)	C ₃₁ $\alpha\beta$ 22S/(22S+22R)	Ts/Tm	γ / $\alpha\beta$ C ₃₀ H ^c
BL-4	nC ₁₇	1.06	1.04	9.4	2.93	0.53	0.51	1.31	0.20	0.71	1.11	0.59	0.58	1.04	0.06
BL-3	nC ₁₆	0.92	Nd	Nd	5.87	0.32	0.54	0.67	0.31	0.40	0.92	0.48	0.59	1.42	0.12
BL-2	nC ₁₆	0.91	1.05	Nd	8.68	0	0.32	0	0.70	0.45	1.33	0.53	0.59	1.12	0.09
BL-1	nC ₁₆	0.94	1.05	17.8	4.05	0.3	0.56	0.7	0.32	0.48	1.11	0.50	0.59	1.86	0.11

^a (C₂₁+6C₂₃+C₂₅)/(4C₂₂+4C₂₄);

^b [2(C₂₃+C₂₅+C₂₇+C₂₉)]/[C₂₂+2(C₂₄+C₂₆+C₂₈)+C₃₀];

^c γ , gammacerane; Nd: no data.

5. Discussion

5.1. Organic richness

The Lower Toarcian oil shales from the Shuanghu area have organic carbon contents of 1.8 to 26.1% with an average of about 8.7% [17, 21]. Generally, the Lower Toarcian oil shales have a good quality organic matter and an excellent oil-generation potential in the study area. In Europe, the TOC patterns show a striking polarity between 5 and 20 wt% [6–7, 15, 26]. The early Toarcian oceanic anoxic event, as defined by both relatively high TOC values and ammonite and nannofossil biostratigraphy, is clearly synchronous across Europe and undoubtedly prove to be so in global context, given its recent investigation in Argentina [12, 26–28]. These observations of elevated organic richness at the Biluo Co section infer increased primary productivity and/or redox conditions in the water column.

5.2. Biological sources

All the oil shales appear to be dominated by marine-derived (mix algal/bacterial) organic matter. *n*-Alkanes occur widely in crude oils and sediments and the distributions often provide information relating to OM origin [29–30]. Accordingly, the short chain *n*-alkanes may indicate an algal/bacterial contribution and the long chain ones could derive from land plants [29]. The oil shales are characterized by a marked predominance of short chain *n*-alkanes with a maximum at C₁₆ or C₁₇, and the nC₁₇/nC₃₁ ratio values between 9.4 and 17.8 (Table), representing the algal/bacterial input,

which is similar to the Toarcian black shales in Europe [23]. Based on OEP (1.04–1.05) and CPI (0.91–1.06) close to 1.0, all the samples showed no distinct odd/even predominance. Wang [31] suggested that the *n*-alkanes without an odd/even predominance indicated two origins for the OM, one bacterial/ microbial waxes, the other land plant waxes through significant biodegradation. So we may conclude that algae/bacteria were the predominant primary producers during deposition of the Toarcian.

A series of C₂₇ and C₂₉–C₃₅ hopanes, maximizing at C₃₀ and C₃₁, are present in all samples which contained minor amounts of gammacerane (Fig. 3), as indicated by gammacerane/C₃₀-17 α -hopane values from 0.06 to 0.12 (Table 1). Furthermore, high concentrations of tricyclic terpanes with C₁₉ to C₃₀ carbons were present, but we detected no components indicating cyanobacteria, such as methyl hopanoids [32]. It is noteworthy that not all cyanobacteria biosynthesize methylhopanoids [33]. However, the steroid mixtures indicate the presence of both regular and rearranged C₂₇–C₃₀ desmethyl- and desmethyl/4-methyl steranes and distribution of desmethyl- (C₂₇>C₂₉>C₂₈>C₃₀) and 4-methyl steranes exhibit no major differences among the samples, and the C₂₇/C₂₉ ratios are higher than 1.1, except for 0.92 in sample BL-2, which probably reflects a significant algal contribution.

5.3. Organic matter maturity

The maturity of the sedimentary organic matter is illustrated in this paper by the extent of hopane and sterane side-chain isomerization reactions. Thus, ratios of isomers give an insight into the level of maturity [34]. Ts/(Ts+Tm) values are commonly used to evaluate maturity, with higher values indicating higher maturity [35]. Table 1 shows Ts/(Ts+Tm) values fluctuating between 1.04 and 1.86. Further biomarker maturity parameters are 22S/(22S+22R) C₃₁ $\alpha\beta$ -homohopane, 20S/(20S+20R) $\alpha\alpha\alpha$ and 20R $\alpha\beta\beta$ /($\alpha\alpha\alpha$ + $\alpha\beta\beta$) C₂₉ steranes [29, 35]. The homohopane 22S/(22S+22R) values in this study are all > 0.58 and the sterane 20S/(20S+20R) values are all between 0.48 and 0.59 (Table 1), being consistent with a higher level of thermal maturity.

5.4. Depositional conditions

The environmental conditions that led to the deposition of Toarcian black shales are still being debated. Traditionally, these shales have been interpreted as the product of pelagic settling of organic and inorganic particulate material in anoxic, stagnant bottom waters of silled basins similar to the present-day Black Sea [4, 13, 36–38], but compare Tyson [39] for a discussion on why the Black Sea is a poor analogue. However, evidence for benthic colonization events at certain horizons within these shales [40–42] and for high-energy events in the water column and benthic zone [43] has led to a considerable debate about whether the water column was anoxic at all and, if so, on whether anoxia was ever persistent. Trabucho-Alexandre et

al. [5] thought the lower Toarcian black shales in the Dutch Central Graben exhibit a variety of depositional fabrics, sedimentary structures, and textures that indicate dynamic energetic conditions at the time of their deposition and appear to have been deposited mostly by bottom currents rather than settling from pelagic suspension.

The geochemical parameters indicate the depositional conditions such as Pr/Ph, gammacerane, and steranes. The low Pr/Ph ratio values suggest an origin from sediments deposited under anoxic conditions and, likely, under stratified water columns [44]. Empirical evidence suggests that the Pr/Ph value < 0.8 is diagnostic for anoxic environments, as commonly encountered in strongly stratified water columns [29]. The samples in the lower part have low Pr/Ph values from 0.67 to 0.7, in the upper part 1.31, which indicates from lower to upper of this section, bottom water conditions changed from anoxic to slightly more oxygenated environments.

In addition, the significant abundance of gammacerane, a series of 17(21)-homohopanes extending to C₃₅ with complete isomerization at the C-22 site, and the presence of 5 α (H), 14 β (H), 17 β (H)-steranes indicate hypersaline conditions [44]. However, all samples show low abundance of the above-mentioned molecular gammacerane, a series of 17(21)-homohopanes, and the gammacerane/hopane values were around 0.06 to 0.12, which would be consistent with black shale deposition at normal marine salinity.

5.5. The mechanisms of carbon isotope excursion

Much attention has focused on the events surrounding the Early Toarcian Oceanic Anoxic Event (OAE: c. 183–175.6 Ma) in the Early Jurassic [5, 10]. The relative enrichment with organic matter of certain Lower Toarcian strata, together with the marine and terrestrial carbon-isotope record, indicates that a large perturbation in the carbon cycle took place at that time [8]. The Toarcian black shales are associated with a pronounced (c. 7%) negative (organic) carbon isotope excursion (CIE) which is thought to be the result of a major perturbation in the global carbon cycle [2, 13, 36, 45]. Indeed, black shale deposition, while favored by global mechanisms, is ultimately dependent on local processes and conditions (e.g., Trabucho-Alexandre et al. 2011) [46].

The Lower Toarcian oil shales from the Shuanghu area are characterized by the $\delta^{13}\text{C}_{\text{kerogen}}$ fluctuating from -26.22 to -23.53% PDB with a positive excursion close to 2.17% . According to the C/N ratios, the present studies indicate that the carbon-isotope excursion has been ascribed to the sea level and palaeoproductivity [17]. Through this study, we show that biomarker distributions differ only slightly among the samples, which strongly suggests that differences in $\delta^{13}\text{C}_{\text{kerogen}}$ are related to the difference in $\delta^{13}\text{C}$ of CO₂ in the photic zone. Therefore, in the Toarcian, the ocean-atmosphere system was subject to one of the largest perturbations of the carbon cycle in the last 250 Myr known as the Toarcian Oceanic Anoxic Event (TOAE) [9]. Widespread anoxia led to the deposition of organic-rich sediments that removed

isotopically light carbon from the oceans and drove carbon-isotope ratios to higher values.

6. Conclusions

All Biluo Co oil shale samples are characterized by the presence of *n*-alkanes, isoprenoids, terpanes and steranes. The biomarker distributions and some important parameters show that all the oil shales appear to be dominated by marine-derived (mix algal/bacterial) organic matter with a higher level of thermal maturity. The Early Toarcian Oceanic Anoxic Event (T-OAE) was a global event of environmental and carbon cycle perturbations which were deeply affected by sea-level fluctuation, palaeoproductivity and the difference in $\delta^{13}\text{C}$ of CO_2 in the photic zone.

Acknowledgements

We thank Maocheng Wang, Guoqing Xia, Chihua Wu and other researchers for field investigations. This research was financed by the National Natural Science Foundation of China (grants No. 41102066, 40972084) and the Opening Foundation of the State Key Laboratory of Ore Deposit Geochemistry, Institute of Geochemistry, Chinese Academy of Sciences.

REFERENCES

1. Jenkyns, H. C. Geochemistry of oceanic anoxic event. *Geochem. Geophys. Geosy.*, 2010, **11**(3), 1–30.
2. Schouten, S., van Kaam-Peters, H. M. E., Rijpstra, W. I. C., Schoell, M., Sinninghe Damste, J. S. Effects of an oceanic anoxic event on the stable carbon isotopic composition of early Toarcian carbon. *Am. J. Sci.*, 2000, **300**(1), 1–22.
3. Barnard, P. C., Cooper, B. S. Oils and source rocks of the North Sea area. In: *Petroleum Geology of the Continental Shelf of North-West Europe: proceedings of the second Conference on Petroleum Geology of the Continental Shelf of North-West Europe* (Illing, L. V., Hobson, G. D, eds.). Institute of Petroleum (Great Britain), 1981, 169–175.
4. McArthur, J. M., Algeo, T. J., Van de Schootbrugge, B., Li, Q., Howarth, R. J. Basinal restriction, black shales, Re-Os dating, and the Early Toarcian (Jurassic) oceanic anoxic event. *Paleoceanography*, 2008, **23**(4), PA4217, doi:10.1029/2008pa001607.
5. Trabucho-Alexandre, J., Dirkx, R., Veld, H., Klaver, G., De Boer, P. L. Toarcian black shales in the Dutch Central Graben: record of energetic, variable depositional conditions during an oceanic anoxic event. *J. Sediment. Res.*, 2012, **82**(2), 104–120.

6. Jenkyns, H. C., Clayton, C. J. Lower Jurassic epicontinental carbonates and mudstones from England and Wales: chemostratigraphic signals and the early Toarcian anoxic event. *Sedimentology*, 1997, **44**(4), 687–706.
7. Röhl, H. J., Schmid-Röhl, A., Oschmann, W., Frimmel, A., Schwark, L. The Posidonia Shale (Lower Toarcian) of SW-Germany: an oxygen-depleted ecosystem controlled by sea level and palaeoclimate. *Palaeogeogr. Palaeoclimatol.*, 2001, **169**(34), 273–299.
8. Littler, K., Hesselbo, S. P., Jenkyns, H. C. A carbon-isotope perturbation at the Pliensbachian–Toarcian boundary: evidence from the Lias Group, NE England. *Geol. Mag.*, 2010, **147**(2), 181–192.
9. Hermoso, M., Minoletti, F., Rickaby, R. E. M., Hesselbo, S. P., Baudin, F., Jenkyns, H. C. Dynamics of a stepped carbon-isotope excursion: Ultra high-resolution study of Early Toarcian environmental change. *Earth. Planet. Sc. Lett.*, 2012, **319–320**, 45–54.
10. Jenkyns, H. C., Clayton, C. J. Black shales and carbon isotopes in pelagic sediments from the Tethyan Lower Jurassic. *Sedimentology*, 1986, **33**(1), 87–106.
11. McArthur, J. M., Donovan, D. T., Thirlwall, M. F., Fouke, B. W., Matthey, D. Strontium isotope profile of the early Toarcian (Jurassic) oceanic anoxic event, the duration of ammonite biozones, and belemnite palaeotemperatures. *Earth. Planet. Sc. Lett.*, 2000, **179**(2), 269–285.
12. Jenkyns, H. C., Jones, C. E., Gröcke, D. R., Hesselbo, S. P., Parkinson, D. N. Chemostratigraphy of the Jurassic System: applications, limitations and implications for palaeoceanography. *J. Geol. Soc. London*, 2002, **159**, 351–378.
13. Hesselbo, S. P., Jenkyns, H. C., Duarte, L. V., Oliveira, L. C. V. Carbon-isotope record of the Early Jurassic (Toarcian) Oceanic Anoxic Event from fossil wood and marine carbonate (Lusitanian Basin, Portugal). *Earth. Planet. Sc. Lett.*, 2007, **253**(3–4), 455–470.
14. Gómez, J. J., Arias, C. Rapid warming and ostracods mass extinction at the Lower Toarcian (Jurassic) of central Spain. *Mar. Micropaleontol.*, 2010, **74**(3–4), 119–135.
15. Pancost, R. D., Crawford, N., Magness, S., Turner, A., Jenkyns, H. C., Maxwell, J. R. Further evidence for the development of photic-zone euxinic conditions during Mesozoic oceanic anoxic events. *J. Geol. Soc. London*, 2004, **161**(3), 353–364.
16. Bowden, S. A., Farrimond, P., Snape, C. E., Love, G. D. Compositional differences in biomarker constituents of the hydrocarbon, resin, asphaltene and kerogen fractions: An example from the Jet Rock (Yorkshire, UK). *Org. Geochem.*, 2006, **37**(3), 369–383.
17. Chen, L., Yi, H. S., Hu, R. Z., Zhong, H., Zou, Y. R. Organic Geochemistry of the Early Jurassic Oil Shale from the Shuanghu Area in Northern Tibet and the Early Toarcian Oceanic Anoxic Event. *Acta Geol. Sin-Engl.*, 2005, **79**(3), 392–397.
18. Li, C., He, Z. H., Yang, D. M. The problems of geological tectonics in the Qiangtang Area, Tibet. *Global Geology*, 1996, **15**(3), 18–23 (in Chinese with English abstract).
19. Matte, P., Tapponnier, P., Arnaud, N., Bourjot, J., Avouac, J. P., Vidal, P., Liu, Q., Pan, Y. S., Wang, Y. Tectonics of Western Tibet, between the Tarim and the Indus. *Earth. Planet. Sc. Lett.*, 1996, **142**(3–4), 311–330.

20. Chen, L., Lin, A. T.-S., Da, X. J., Yi, H. S., Tsai, L. L.-Y., Xu, G. W. Sea-level changes recorded by cerium anomalies in the Late Jurassic (Tithonian) black rock series of Qiangtang Basin, north-central Tibet. *Oil Shale*, 2012, **29**(1), 18–35.
21. Lin, J. H., Yi, H. S., Li, Y., Wang, C. S., Peng, P. A. Characteristics of biomarker compounds and its implication of Middle Jurassic oil shale sequence in Shuanghu Area, Northern Tibet Plateau. *Acta Sedimentol. Sinica*, 2001, **19**(2), 287–292 (in Chinese with English abstract).
22. Farrimond, P., Eglinton, G., Brassell, S. C., Jenkyns, H. C. The Toarcian black shale event in northern Italy. *Org. Geochem.*, 1988, **13**(4–6), 823–832.
23. Farrimond, P., Eglinton, G., Brassell, S. C., Jenkyns, H. C. Toarcian anoxic event in Europe: an organic geochemical study. *Mar. Petrol. Geol.*, 1989, **6**(2), 136–147.
24. Farrimond, P., Talbot, H. M., Watson, D. F., Schulz, L. K., Wilhelms, A. Methylhopanoids: Molecular indicators of ancient bacteria and a petroleum correlation tool. *Geochim. Cosmochim. Ac.*, 2004, **68**(19), 3873–3882.
25. Blanc, P., Connan, J. Origin and occurrence of 25-norhopanes: a statistical study. *Org. Geochem.*, 1992, **18**(6), 813–828.
26. Sabatino, N., Neri, R., Bellanca, A., Jenkyns, H. C., Baudin, F., Parisi, G., Masetti, D. Carbon-isotope records of the Early Jurassic (Toarcian) oceanic anoxic event from the Valdorbia (Umbria–Marche Apennines) and Monte Mangart (Julian Alps) sections: palaeoceanographic and stratigraphic implications. *Sedimentology*, 2009, **56**(5), 1307–1328.
27. Palliani, R. B., Mattioli, E., Riding, J. B. The response of marine phytoplankton and sedimentary organic matter to the early Toarcian (Lower Jurassic) oceanic anoxic event in northern England. *Mar. Micropaleontol.*, 2002, **46**(3–4), 223–245.
28. Al-Suwaidi, A., Damborenea, S., Hesselbo, S., Jenkyns, H., Manceñido, M., Riccardi, A. Evidence for the Toarcian oceanic anoxic event in the Southern hemisphere (Los Molles Formation, Neuquén Basin, Argentina). *Geochim. Cosmochim. Ac.*, Goldschmidt Conference Abstracts, 2009, **73**(13), Suppl. 1, A33.
29. Peters, K. E., Walters, C. W., Moldowan, J. M. *The Biomarker Guide: II. Biomarkers and Isotopes in Petroleum Exploration and Earth History*, second ed. Cambridge University Press, Cambridge, 2005.
30. Romero-Sarmiento, M.-F., Riboulleau, A., Vecoli, M., Versteegh, G. J.-M. Aliphatic and aromatic biomarkers from Gondwanan sediments of Late Ordovician to Early Devonian age: An early terrestrialization approach. *Org. Geochem.*, 2011, **42**(6), 605–617.
31. Wang, T. G. A contribution to some sedimentary environmental biomarkers in crude oils and source rocks in China. *Geochemica*, 1990, **19**, 256–263 (in Chinese).
32. Summons, R. E., Jahnke, L. L., Hope, J. M., Logan, G. A. 2-Methylhopanoids as biomarkers for cyanobacterial oxygenic photosynthesis. *Nature*, 1999, **400**, 554–557.
33. Brocks, J. J., Love, G. D., Summons, R. E., Knoll, A. H., Logan, G. A., Bowden, S. A. Biomarker evidence for green and purple sulphur bacteria in a stratified Palaeoproterozoic sea. *Nature*, 2005, **437**, 866–870.
34. Hermann, E., Hochuli, P. A., Méhay, S., Bucher, H., Brühwiler, T., Ware, D., Hautmann, M., Roohi, G., Ur-Rehman, K., Yaseen, A. Organic matter and

- palaeoenvironmental signals during the Early Triassic biotic recovery: The Salt Range and Surghar Range records. *Sediment. Geol.*, 2011, **234**(1–4), 19–41.
35. Seifert, W. K., Moldowan, J. M. Applications of steranes, terpanes and monoaromatics to the maturation, migration and source of crude oils. *Geochim. Cosmochim. Ac.*, 1978, **42**(1), 77–95.
 36. Pye, K., Krinsley, D. H. Microfabric, mineralogy and early diagenetic history of the Whitby Mudstone Formation (Toarcian), Cleveland Basin, U.K. *Geol. Mag.*, 1986, **123**(3), 191–203.
 37. Hesselbo, S. P., Gröcke, D. R., Jenkyns, H. C., Bjerrum, C. J., Farrimond, P., Bell, H. S. M., Green, O. R. Massive dissociation of gas hydrate during a Jurassic oceanic anoxic event. *Nature*, 2000, **406**, 392–395.
 38. Pearce, C. R., Cohen, A. S., Coe, A. L., Burton, K. W. Changes in the extent of marine anoxia during the Early Jurassic: Evidence from molybdenum isotopes. *Geochim. Cosmochim. Ac.*, Goldschmidt Conference Abstracts, 2006, **70**(18), Suppl., A476.
 39. Tyson, R. V. The “productivity versus preservation” controversy: cause, flaws, and resolution. In: *The Deposition of Organic-Carbon-Rich Sediments: Models, Mechanisms, and Consequences* (Harris, N. B., ed.), SEPM Special Publications, 2005, **82**, 17–33.
 40. Kauffman, E. G. Benthic environments and paleoecology of the Posidonien-schiefer (Toarcian). In: *Neues Jahrbuch für Geologie und Paläontologie Abhandlungen*, 1978, **157**, 18–36.
 41. Morris, K. A. A classification of Jurassic marine shale sequences: An example from the Toarcian (Lower Jurassic) of Great Britain. *Palaeogeogr. Palaeocl.*, 1979, **26**, 117–126.
 42. Wignall, P. B. *Black Shales*. Oxford University Press, Oxford, England, 1994, 127.
 43. O’Brien, N. R. Significance of lamination in Toarcian (Lower Jurassic) shales from Yorkshire, Great Britain. *Sediment. Geol.*, 1990, **67**(1–2), 25–34.
 44. Ten Haven, H. L., De Leeuw, J. W., Rullkötter, J., Sinninghe Damsté, J. S. Restricted utility of the pristane/phytane ratio as a palaeoenvironmental indicator. *Nature*, 1987, **330**, 641–643.
 45. Van Breugel, Y., Baas, M., Schouten, S., Mattioli, E., Sinninghe Damsté, J. S. Isorenieratane record in black shales from the Paris Basin, France: Constraints on recycling of respired CO₂ as a mechanism for negative carbon isotope shifts during the Toarcian oceanic anoxic event. *Paleoceanography*, 2006, **21**(4), PA4220.
 46. Trabucho Alexandre, J., Van Gilst, R. I., Rodríguez-López, J. P., De Boer, P. L. The sedimentary expression of oceanic anoxic event 1b in the North Atlantic. *Sedimentology*, 2011, **58**(5), 1217–1246.

Presented by V. Kalm

Received November 19, 2012